The Application of Three Dimensional Finite Volume Methods to the Modelling of Welding Phenomena

G. A. Taylor, M. Hughes and K. Pericleous

Centre for Numerical Modelling and Process Analysis,
University of Greenwich, London, UK

Tel: (44/0)181 331 8702, Fax: (44/0)181 331 8665,
E-mail: physica@gre.ac.uk

Abstract

A three dimensional numerical framework for the computational modelling of welding phenomena is presented. The framework includes models from both the fields of Computational Fluid Dynamics (CFD) and Computational Solid Mechanics (CSM). With regard to the computational modelling of the weld pool fluid dynamics, heat transfer and phase change, cell-centred Finite Volume (FV) methods are employed. Alternatively, novel vertex-based FV methods are employed with regard to the thermo-elasto-plastic deformation associated with the CSM. The FV methods are included within an integrated modelling framework, which can be readily applied to unstructured meshes. The modelling techniques are validated against a variety of reference solutions.

Introduction

Essential to the concept of a welding process is the application of a localised heat source in order to minimise the size of the heat affected zone (HAZ) and therefore reduce unwanted effects such as residual stress and distortion [7]. Traditionally, the modelling of welding phenomena either focuses on the complex fluid and thermo- dynamics local to the weld pool [13],[18],[21] or the global thermo-mechanical behaviour of the weld structure [12],[10]. In the former case only the local geometry of the weld pool and HAZ is considered [13],[18],[21] and in the latter case a simplified heat source model is employed with heat transfer by conduction only [12],[7],[10]. This is reasonable as the length scales involved can differ by several orders of magnitude when application areas such as ship construction are considered [6],[7]. A variety of simplified heat source models are now frequently employed in the simulation of welding processes, but they are totally reliant on the accuracy of the model parameters which describe the weld pool size and shape [12],[7]. The parameters are obtained from a combination of experimental and calculated data. The scientific and engineering software PHYSICA [15] is a numerical modelling framework which can be employed to model 3D industrial and environmental applications. The numerical framework consists of both cell-centred and vertex-based FV methods [3],[17], which are employed to model problems in CFD and CSM, respectively. These procedures can be readily applied to problems involving complex interactions of physical behaviour over arbitrarily unstructured domains and detailed descriptions of their implementations are available [3],[17],[20]. For these reasons, the comprehensive modelling of welding phenomena is ideal for demonstrating the versatility of the modelling framework.

The ultimate aim of this research is the estimation and verification of the parameters associated with the simplified heat source models in order to achieve consistency between the predictions of the two modelling approaches. It may then be possible to transfer thermal data between analyses of the weld pool and the welded structure via the model parameters.

In this paper we will briefly present the modelling of physical phenomena using both approaches. With regard to the thermo-dynamics of the weld pool, surface tension will be accounted for via the inclusion of Marangoni effects [18] and with regard to the thermo-mechanical behaviour of the welded structure, the thermo-elasto-plastic distortion of a butt-welded pipe will be considered [12],[9].

Model Descriptions

The models available in PHYSICA are organised in a modular fashion as illustrated in Figure1 and the relevant models for the simulation of welding processes are now described.

Fluid Dynamics and Heat Transfer

The governing equations for the incompressible fluid flow and heat transfer that can occur in the weld pool are defined as follows;

Mass conservation, $\nabla \cdot \mathbf{u} = 0$, momentum conservation,

$$\rho \frac{\partial \mathbf{u}}{\partial t} + \rho \nabla \cdot (\mathbf{uu}) = -\nabla p + \nabla . \mu \nabla \mathbf{u} + \mathbf{S}_{\mathrm{u}} \qquad (1)$$

and heat conservation,

$$\rho C_p \frac{\partial T}{\partial t} + \rho C_p \nabla . (\mathbf{u}T) = \nabla . (k \nabla T) + S_T . \qquad (2)$$

The Darcy and bouyancy source terms are included in equation (1), respectively, as follows;

$$\mathbf{S}_{\mathrm{u}} = -\frac{\mu}{K} \mathbf{u} + \rho_0 \alpha \mathbf{g} (T - T_0),$$

where K is calculated from the Karman-Kozeny equation [13], ρ_0 is the reference density, α is the thermal expansion coefficient, $\mathbf{g}$ is the gravity and T_0 is the reference temperature.
The latent heat source terms are included in equation (2) as follows [13];

$$S_T = -\rho \frac{\partial(f_l L)}{\partial t} - \rho \nabla.(\mathbf{u} f_l L),$$

where f_l is the liquid metal fraction and L is the latent heat of fusion. The above models are included with the flow, heat and solidification modules of PHYSICA as illustrated schematically in Figure 1.

Surface Tension Boundary Condition

The surface of the weld pool is subjected to the following flow boundary condition [20],[13];

$$\tau.\mathbf{n} = \nabla_s s = \frac{\partial s}{\partial T} \nabla_s T,$$

where τ is the flow stress tensor, $\mathbf{n}$ is the unit normal of the liquid metal surface, s is the temperature dependent surface tension and is ∇_s the surface gradient operator [20]. In this research the derivative of surface tension with regard to temperature is specified as a model parameter and the curvature effects are neglected as a flat weld pool surface is assumed. The surface tension boundary condition is included within PHYSICA via user access to the sources as illustrated in Figure 1.

Solid Mechanics

Incrementally, the quasi-static equation of equilibrium is $\mathbf{L}^T(\Delta\sigma) + \mathbf{b} = \mathbf{0}$, where $\mathbf{L}$ is the differential operator and $\mathbf{b}$ is the body force. The incremental stress-strain relationship can be defined as follows; $\Delta\sigma = \mathbf{D}\Delta\varepsilon_e$, where $\mathbf{D}$ is the elasticity matrix. With regard to the deformation of metals the von-Mises yield criterion is employed and the elastic strain is given by $\Delta\varepsilon_e = \Delta\varepsilon - \Delta\varepsilon_{vp} - \Delta\varepsilon_T$, where $\Delta\varepsilon$, $\Delta\varepsilon_{vp}$, and $\Delta\varepsilon_T$ are the total, visco-plastic and thermal strain, respectively. The visco-plastic strain rate is given by the Perzyna model [14]

$$\frac{d}{dt}\varepsilon_{vp} = \gamma \left\langle \frac{\sigma_{eq}}{\sigma_y} - 1 \right\rangle^{1/N} \frac{3}{2\sigma_{eq}} \mathbf{s},$$

where σ_{eq}, σ_y, γ, N, and $\mathbf{s}$ are the equivalent stress, yield stress, fluidity, strain rate sensitivity parameter and deviatoric stress, respectively. The mathematical operator is defined as follows;

$$\langle x \rangle = \begin{cases} 0 & \text{when} \quad x \leq 0 \\ x & \text{when} \quad x > 0 \end{cases}.$$

The increment of total infinitesimal strain is $\Delta\varepsilon = \mathbf{L}\Delta\mathbf{d}$, where $\Delta\mathbf{d}$ is the incremental displacement. The above solid mechanics capabilities are included within PHYSICA via the EVP module as illustrated in Figure 1 and are coupled with the heat transfer modules in a staggered incremental fashion [17].

Simplified Heat Source Models

The simplified heat source models that are employed in this paper are as follows; Firstly, the Gaussian heat source over a surface in the y plane [12]

$$q(x,z,t) = \frac{3Q}{\pi r^2} e^{-3\left(\frac{\Delta x - v_x t}{r}\right)^2} e^{-3\left(\frac{\Delta z - v_z t}{r}\right)^2}, \tag{3}$$

where Q, r and v are the heat input, characteristic length and velocity weld parameters, respectively. Secondly, the double ellipsoidal heat source over a volume [7]

$$q(x,y,z,t) = \frac{6\sqrt{3} f_w Q}{abc\,\pi\sqrt{\pi}} e^{-3\left(\frac{\Delta x - v_x t}{a}\right)^2} e^{-3\left(\frac{\Delta y - v_y t}{b}\right)^2} e^{-3\left(\frac{\Delta z - v_z t}{c}\right)^2}, \tag{4}$$

where f_w are weighting fractions associated with each ellipsoid, a, b and c are the axes of the ellipses. In both cases $\Delta x = x - x_0$, $\Delta y = y - y_0$ and $\Delta z = z - z_0$ are coordinates relative to the original location of the heat source, which is moving with a constant weld velocity (v_x, v_y, v_z).

Both models are also included within PHYSICA via user access to the sources, as illustrated in Figure 1.

Results

A selection of results obtained from a variety of welding related problems is presented. The various problems employ the models defined in the previous section.

Thermo-mechanical Analysis of a Girth Weld

The residual effective stress field as calculated for a girth welding process of a thin pipe is illustrated in Figure 2. Assuming symmetry along the weld line, only half the structure is modelled. The residual stress contours (MPa) are plotted on the deformed shape (Mag. x100) after 1,000 seconds and are in good agreement with the original analysis [12]. The girth welding sequence involved one pass, starting and finishing at the 12 o'clock position, and lasted 89 seconds [12],[9]. In this case, the moving heat source can be modelled as a point source moving on the external surface of the pipe [12]. For this analysis a cylindrical polar mapping of equation (3) was employed. The thermo-elasto-plastic analysis was performed in a staggered incremental fashion [17]. Equivalent spatial and temporal discretisation was employed to that of the original analysis [12]. The temperature dependent material properties for the thermal and mechanical analyses are equivalent to those used in the original analysis [12]. However, for the simulation presented in this paper the effects of metallurgical phase transitions were neglected. The temperature profiles at locations on the outer surface of the pipe are illustrated in Figure 3 and are in reasonable agreement with the experimental measurements of Jonsson and Josefson [9]. The hoop stress profile at a location close to the weld path is illustrated in Figure 4 and is in good agreement with the calculations of Lindgren and Karlsson with regard to the initial thermal response. However, the predicted residual stress is approximately 30% greater, this may be attributable to the neglection of phase transformations and the use of 8 noded brick elements as opposed to shell elements [12].

Comparison of Simplified Heat Source Models

Results obtained using the simple heat source models described by equations (3) and (4) are illustrated in Figure 5. When they were proposed, both these models were originally compared against the experimental data of Christensen *et al*. [2]. The temperature profiles illustrated in Figure 5 are plotted perpendicular to the direction of the weld line, 11.5 seconds after the heat source has passed. The results obtained from PHYSICA are in close agreement with the original results obtained for both models and illustrate again the closer agreement of the ellipsoidal model proposed by Goldak *et al*. [7] with regard to the experimental results. The lack of accuracy of the surface model employed by Krutz and Segerlind [11] has been demonstrated with regard to certain welding applications, ie. deep penetration electron or laser beam welding [7], where the digging action of the heat source is not captured. It is important to note that both models require a modified value of conductivity in the weld pool during the liquid phase [11],[7]. This is to account for the possible transfer of heat by convection. The accuracy of the numerical analyses employing these models is very sensitive to the conductivity and therefore a thorough understanding of the weld pool thermodynamics is required in order to modify the conductivity values correctly.
The ultimate aims of this research are to determine heat source model parameters and modified values of conductivity that are consistent with the predicted thermodynamics of particular weld pools.

Marangoni Convection in Weld Pools

Two problems will be considered. The first case is the motion of a liquid resulting from a free surface, where the surface tension is quadratically dependent on temperature [8]. The

second case is the inclusion of Marangoni effects in the axisymmetric modelling of weld pools [18]. In both cases reference solutions are available.

Case 1: The thermo-capillary motion of an idealised liquid with surface tension as a quadratic function of temperature is considered. The boundary conditions required for the thermo-capillary analysis are illustrated in Figure 6. In this analysis a 10 by 0.4 aspect ratio is employed with regard to the geometry. Thus permitting the application of a symmetry condition at a finite distance from the region of interest. The region of interest is the cross section x-s, which is close to the boundary $T = T_0$, see Figure 6. The constants β and a, define the quadratic relationship of surface tension s to temperature T, and the linear variation of temperature and spatial coordinate X, respectively. The resultant velocity component profiles are plotted in Figures 7 and 8, along the cross section x-s illustrated in Figure 6. The results are in good agreement with the analytical solution [8].

Case 2: The stationary and steady state fusion of an aluminium plate by a heat source defined over a surface is considered. The model for the steady state heat source distribution is obtained from equation (3) as follows;

$$q(x) = \frac{\sqrt{3}Q}{\sqrt{\pi}r} \, e^{-3\left(\frac{\Delta x - v_x t}{r}\right)^2} \, .$$

An axisymmetric approximation is assumed, and convective and radiative heat loss boundary conditions applied on remainder of the surface, $x > r$. To enable a localised analysis, it is assumed that the boundary conditions away from the axis and surface can be derived from the analytical solution for an equivalent point heat source [16]. The results from the numerical analysis are illustrated in Figures 9a and 10a with regard to a negative and positive surface tension gradient, $-.35 \times 10$ and $.1 \times 10^{-3}$ kg/(s^{2}K) respectively. The two gradient values represent different types of alloy and demonstrate the different Marangoni effects on the velocity and temperature fields. The temperature fields are contoured in degrees Celsius and as illustrated by Figure 9a the shape of the weld pool is flatter for the negative gradient case. The change in weld pool shape is related to the different flow patterns that occur in each weld pool, as illustrated in Figures 9a and 10a. For the negative or positive gradient case the predominant flow is away from or towards the heat source, respectively. In this way the convective heat transport is directed towards or away from the axis, resulting in either a deeper or flatter weld pool shape, respectively. The results are in good agreement with those obtained by Tsai and Kou [18], which are represented in Figures 9b and 10b. The results for the negative case are in general agreement with regard to weld pool shape, temperature field and flow field as illustrated in Figures 9a and 9b. Additionally, the results for the positive case are also generally in good agreement as illustrated in Figures 10a and 10b. Although it should be noted that in the positive case PHYSICA predicts a slightly deeper weld pool shape.

Further Research

At present there are a number of methods for modelling welding processes depending upon the reference frame associated with the heat source. Essentially, the methods are Eulerian, where the heat source is stationary [1],[6], or Lagrangian, where the heat source is moving [19],[4]. The methods employed in this paper for welding processes involving a moving heat source are an implementation of the Lagrangian approach. This approach is reasonably accurate for simplified heat sources moving with a constant velocity [5], but it is not suitable when modelling the fluid dynamics of a weld pool associated with a moving heat source. Therefore, further research will involve the development of Eulerian techniques within PHYSICA, which will facilitate the localised modelling of the fluid dynamics associated with a moving weld pool. Additional further research will involve the inclusion of Lorentz effects, which are necessary for modelling arc welding processes, where electro-magnetic fields can exist and interact with the fluid dynamics of the weld pool. With regard to global thermo-mechanical analyses of a welded structure, further research will include the introduction of metallurgical phase transformations and the addition of filler material [4],[19]. It should be

noted that the thermo-mechanical analyses have been performed using Eulerian and Lagrangian frames of reference for the heat source and mechanical behaviour, respectively [6]. However, the Eulerian approach is not generally suitable for the welding of large structures, particularly when welding sequences are involved. This is because the local mechanical constraints do not necessarily reflect the global mechanical behaviour. For these reasons most thermo-mechanical analyses of the welding of large structures involve the former technique [4],[19].

References

[1] Chen, X., Becker, M., and Meekisho, L., (1998), "Welding analysis in moving coordinates.", In H. Cerjak, Editor, *Mathematical Modelling of Welding Phenomena 4*, 396-410.

[2] Christensen, N., Davies, V. De L. and Gjermundsen, K., (1965), "Distribution of temperatures in arc welding", *British Welding Journal*, **12**, 54-75.

[3] Croft, T. N., (1998), "Unstructured mesh – finite volume algorithms for swirling, turbulent, reacting flows.", PhD thesis, The University of Greenwich.

[4] Feng, Z., Cheng, W. and Chen, Y., (1998), "Development of new modeling procedures for 3D welding residual stress and distortion assessment.", *Cooperative Research Program*, **SR9818**.

[5] Goldak, J., Bibby, M., Moore, J., House, R. and Patel B., (1986), "Computer Modelling of Heat Flow in Welds.", *Met. Trans. B,* **17B**, 587-600*.*

[6] Goldak, J., Breiguine, V. and Dai, N., (1995), "Computational Weld Mechanics: A Progress Report on Ten Grand Challenges", In H. B. Smartt, J. A. Johnson and S. A. David, editors, *Trends in Welding Research – IV*, 5-11.

[7] Goldak, J., Chakravarti, A. and Bibby, M., (1984), "A New Finite Element Model for Welding Heat Sources", *Met. Trans. B*, **15B**, 299-305.

[8] Gupalo, Y. P. and Ryazantsev, Y. S., (1989), "Thermocapillary motion of a liquid with a free surface with nonlinear dependence of the surface tension on the temperature", *Fluid Dynamics,* (English translation), **23:5**, 752-757.

[9] Jonsson M. and Josefson B. L., (1988), "Experimentally Determined Transient and Residual Stresses in a Butt-Welded Pipe", *Journal of Strain Analysis for Engg. Design,* **23**, 25-31.

[10] Kiselev, S. N., Kiselev, A. S., Kurkin, A. S., Aladinskii, V. V. and Makhanev, V. O., (1999), "Current Aspects of Computer Modelling Thermal and Deformation Stresses and Structure Formation in Welding and Related Technologies", *Welding International* , **13-4**, 314-322.

[11] Krutz, G. W. and Segerlind, L. J., (1978), "Finite element analysis of weld structures", *Welding Research Supplement*, **57**, 211s-216s.

[12] Lindgren L.-E. and Karlsson L., (1988), "Deformations and Stresses in Welding of Shell Structures", *Int. J. Num. Methods in Engg.,* **25**, 635-655.

[13] Pericleous, K. and Bailey, C., (1995), "Study of Marangoni phenomena in laser-melted pools". In J. Campbell and M. Cross, editors, *Modeling of Casting, Welding and Advanced Solidification Processes - VII*, 91-100.

[14] Perzyna, P., (1966), "Fundamental problems in visco-plasticity.", *Advan. Appl. Mech.*, **9**, 243-377.

[15] Physica, MPS Ltd., 5 The Priors, Harriots Lane, Ashtead, Surrey, UK.

[16] Rosenthal, D., (1946), "The Theory of Moving Sources of Heat and Its Application to Metal Treatments.", *Trans. ASME*, **68-11**, 849-866.

[17] Taylor, G. A, (1996), "A vertex based discretisation scheme applied to material non-linearity within a multi-physics finite volume framework.", PhD thesis, The University of Greenwich.

[18] Tsai, M. C. and Sindou Kou, (1989), "Marangoni convection in weld pools with a free surface", *Int. J. Num. Methods Engrg.*, **9**, 1503-1516.

[19] Voss, O., Decker, I. and Wohlfahrt, H., (1998), "Consideration of microstructural transformations in the calculation of residual stresses and distortion of larger weldments.", In H. Cerjak, Editor, *Mathematical Modelling of Welding Phenomena 4*, 584-596.

[20] Wheeler, D., Bailey, C. and Cross, M., (1999), "Numerical modelling and Validation of Marangoni and Surface Tension Phenomena Using the Finite Volume Method", *Int. J. Num. Methods in Fluids,* **212-B**, accepted for publication.

[21] Zacharia T., David, S. A., Vitek J. M. and Kraus H. G., (1991), "Computational modelling of stationary gas-tungsten-arc weld pools and comparison to stainless steel 304 experimental results", *Met. Trans B,* **22B**, 243-257.
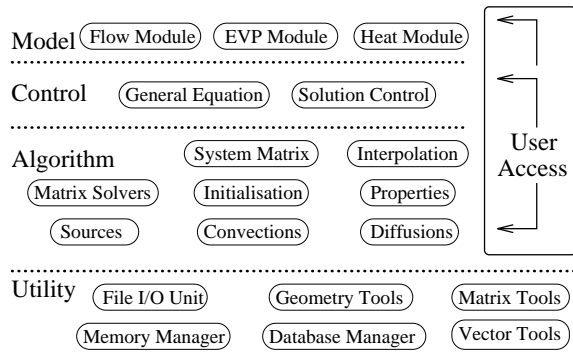
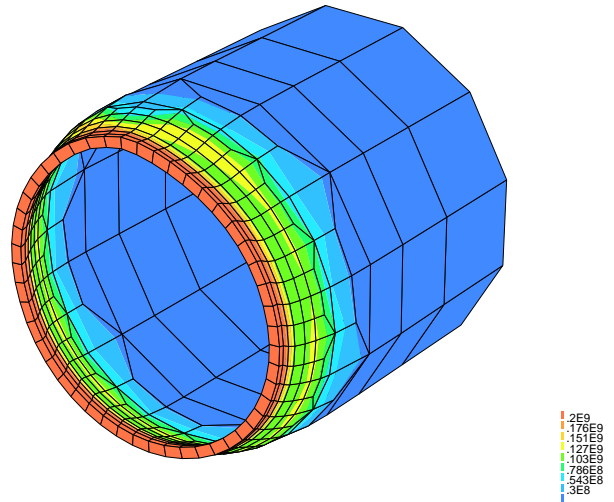**Figure 1:** Abstract diagram of PHYSICA
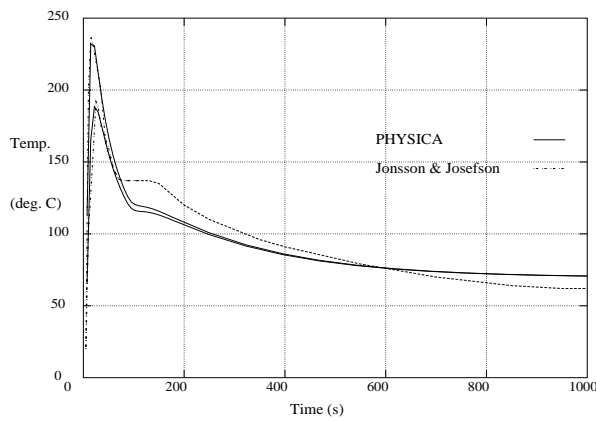

Figure 2: Girth welding of a thin pipe

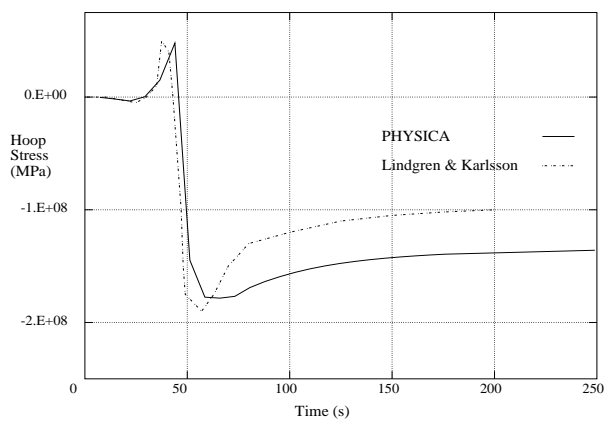**Figure 3:** Surface temperatures of pipe

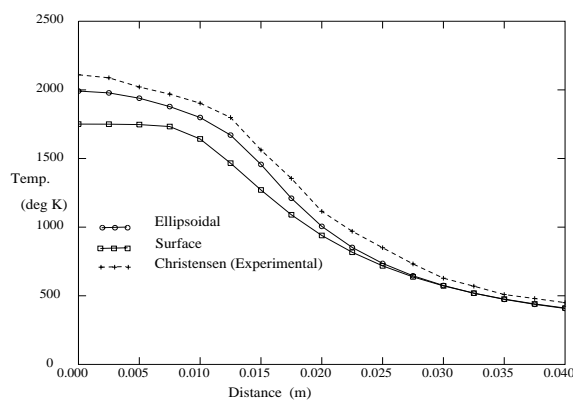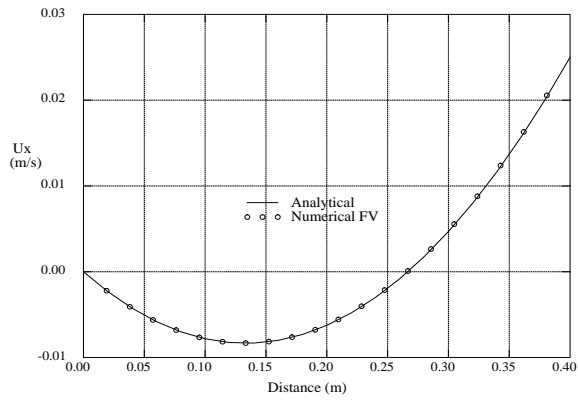**Figure 4:** Residual stress in pipe
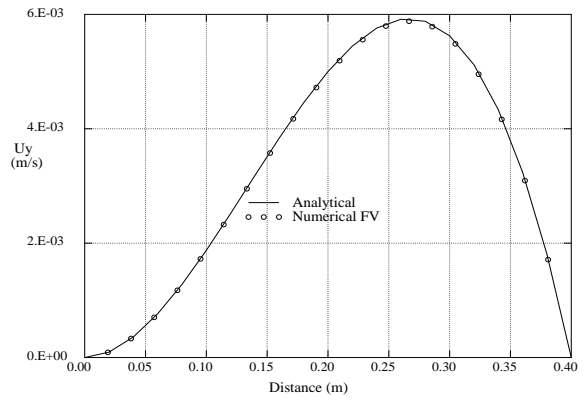

Figure 5: Temperature profiles after 11.5 s.

$$\frac{\partial T}{\partial Y} = 0, \quad \mu\rho\frac{\partial u_X}{\partial Y} = \frac{\partial s}{\partial X} = \beta(T - T_0)\frac{\partial T}{\partial X}$$

$T = T_0$ x-s $(X = .625\text{m})$ Symmetry

Y $X = 0$ $X = 10$

$T = T_0 + aX, \quad u_X = u_Y = 0$
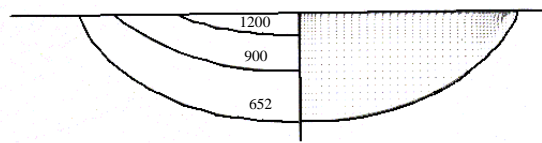
X

Figure 6: Thermo-capillary conditions

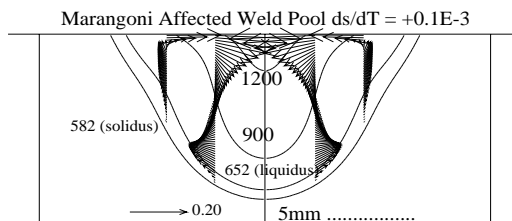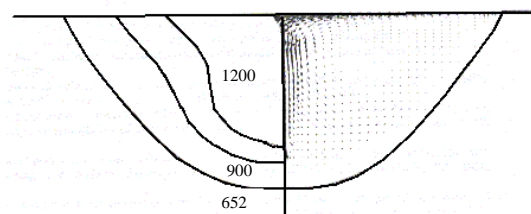**Figure 7:** X component velocity profile   **Figure 8:** Y component velocity profile
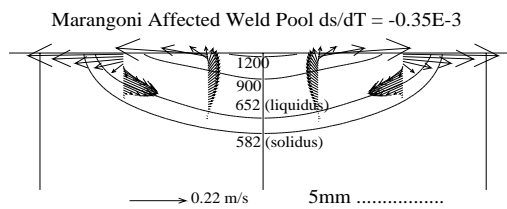
Figure 9a: Negative: Temperature and flow fields.

Figure 9b: Negative: Temperature and flow fields [18]

Figure 10a: Positive: Temperature and flow fields.

Figure 10b: Positive: Temperature and flow fields [18]